Excitation Transfer for K_2 in High-Lying States by N_2 *

CUI Xiu-Hua(崔秀花)[1,2], MU Bao-Xia(穆保霞)[1,2], DAI Kang(戴康)[2], SHEN Yi-Fan(沈异凡)[2]**

[1]*School of Science, Xi'an Jiaotong University, Xi'an 710049*
[2]*Department of Physics, Xinjiang University, Urumqi 830046*

(Received 15 April 2010)

A K-N_2 mixture is irradiated in a glass fluorescence cell with pulses of 710 nm radiation from an OPO laser, populated K_2 ($^1\Lambda_g$) state by two-photon absorption. The cross section for $^1\Lambda_g \to {}^3\Lambda_g$ transfer in K_2 is determined using molecular fluorescence spectrometry. The cell temperature is kept constant at 553 K. The N_2 pressure is varied between 40 Pa and 400 Pa. The effects of K_2-K collisions could not be neglected. These effects are subtracted out by using the results of the pure K experiment. The cross sections are $(3.8 \pm 1.5) \times 10^{-15}\,\mathrm{cm}^2$ for K_2 $(^1\Lambda_g) + N_2 \to K_2(^3\Lambda_g) + N_2$ and $(8.9 \pm 3.5) \times 10^{-15}\,\mathrm{cm}^2$ for K_2 $(^3\Lambda_g)$ collisions with N_2.

PACS: 34. 90. +q, 34. 50. Rk DOI: 10.1088/0256-307X/27/7/073401

Collisional excitation energy transfer (CEET) occurring as a result of the collision between excited atoms or molecules and diatomic molecules has been extensively studied theoretically and experimentally.[1−7] It has been shown that diatomic molecules have rich rovibrational energy levels, which means that the physical and chemical processes of the energy transfer can be more affected.[8−13]

In a mixture of alkali metal and nitrogen vapors, the high-lying states of alkali metal molecules have been obtained by two-photon absorption (due to highly dense energy levels, the middle-level is always found for small detuning). Other excited states of alkali metal molecules can be obtained by collisional energy transfer. In our work, the OPO laser pumped by a YAG laser is tuned to 710 nm to excite K_2 molecules from the ground state $1^1\Sigma_g^+$ to $^1\Lambda_g$ state by two-photon absorption. As shown in Fig. 1, $^1\Lambda_g$ identifies the $8^1\Sigma^+$ or $4^1\Pi_g$ state, which have the almost same electronic state energy levels, 28149 cm^{-1} and 28136 cm^{-1}, respectively.[14]

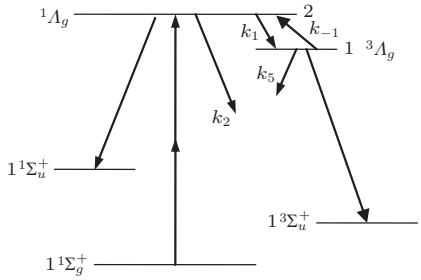

Fig. 1. Processes involved in the population and depopulation of K_2 levels in the experiment.

The collision processes between the $^1\Lambda_g$ state and N_2 are expressed as

$$K_2(^1\Lambda_g) + N_2 \underset{k_{-1}}{\overset{k_1}{\rightleftharpoons}} K_2(^3\Lambda_g) + N_2, \tag{1}$$

$$K_2(^1\Lambda_g) + N_2 \xrightarrow{k_2} K_2 \text{ other than } K_2(^3\Lambda_g) + N_2, \tag{2}$$

where $^3\Lambda_g$ indicates $6^3\sum_g^+$, $4^3\prod_g$ or $5^3\prod_g$, which have almost the same electronic energy levels 28036, 28048 and 28052 cm^{-1}, respectively;[14] k is the rate coefficient. These states can all transit to the same lower energy level $1^3\sum_u^+$ and the corresponding spectral bands will overlap with each other. Therefore, these states are considered to be the same energy level. In addition, the collisional energy transfer between the K_2 $(^1\Lambda_g)$ state and the ground state of the potassium atom could not be neglected, since the following processes should also be considered.

$$K_2(^1\Lambda_g) + K \underset{k_{-3}}{\overset{k_3}{\rightleftharpoons}} K_2(^3\Lambda_g) + K, \tag{3}$$

$$K_2(^1\Lambda_g) + K \xrightarrow{k_4} K_2 \text{ other than } K_2(^3\Lambda_g) + K, \tag{4}$$

In addition to transferring to $^1\Lambda_g$, $^3\Lambda_g$ also transfers to other states such as

$$K_2(^3\Lambda_g) + N_2 \xrightarrow{k_5} K_2 \text{ states other than } K_2(^1\Lambda_g) + N_2, \tag{5}$$

$$K_2(^3\Lambda_g) + K \xrightarrow{k_6} K_2 \text{ states other than } K_2(^1\Lambda_g) + K. \tag{6}$$

Therefore, processes (2), (4)–(6) should be considered when processes (1) and (3) are studied.

Here we define $n_2(t)$ and $n_1(t)$ to be the population densities of the $^1\Lambda_g$ and $^3\Lambda_g$ states, respectively. Then the rate equations are expressed as

$$\frac{d}{dt}n_2(t) = -\frac{n_2}{\tau_2} + \{k_{-1}[N_2] + k_{-3}[K]\}n_1, \tag{7}$$

$$\frac{d}{dt}n_1(t) = -\frac{n_1}{\tau_1} + \{k_1[N_2] + k_3[K]\}n_2, \tag{8}$$

where $[N_2]$ and $[K]$ are the densities of N_2 and K atoms, respectively; τ_2 and τ_1 are the corresponding effective lifetimes. In Eq. (7), $k_{-1}[N_2] + k_{-3}[K]$ are neglected in comparison to $1/\tau_2$ for $k_{-1}[N_2] + k_{-3}[K] \ll 1/\tau_2$, this will be interpreted in detail later. Since $^1\Lambda_g$ is optically excited, the solutions of Eqs. (7) and (8)

*Supported by the National Natural Science Foundation of China under Grant No 10664003.
**To whom correspondence should be addressed. Email: shenyifan01@sina.com;xjcxh0991@sina.cn
© 2010 Chinese Physical Society and IOP Publishing Ltd

under the initial conditions of $n_2(t) = n$ and $n_1(t) = 0$ are written as

$$n_2(t) = ne^{-t/\tau_2}, \tag{9}$$

$$n_1(t) = \frac{\{k_1[\mathrm{N_2}] + k_3[\mathrm{K}]\}n\tau_1\tau_2}{\tau_2 - \tau_1}(e^{-t/\tau_2} - e^{-t/\tau_1}). \tag{10}$$

In the pure K metal cell, the densities of the K atoms change with the changing of the cell temperature. Equations (9) and (10) take the forms

$$n_2'(t) = ne^{-t/\tau_2'}, \tag{11}$$

$$n_1'(t) = \frac{k_3[\mathrm{K}]n\tau_1'\tau_2'}{\tau_2' - \tau_1'}(e^{-t/\tau_2'} - e^{-t/\tau_1'}). \tag{12}$$

The decay signal of the time-resolved fluorescence from the $^1\Lambda_g \to 1^1\sum_u^+$ (650 nm) transition is recorded in the different densities of the K atoms. Here τ_2' could be directly obtained from Eq. (11) in the relevant densities of the K atoms. We notice the Stern–Volmer equation[11]

$$1/\tau_2' = \Gamma_2 + (\sigma_3 + \sigma_4)\upsilon_{\mathrm{K-K_2}}[\mathrm{K}], \tag{13}$$

where $1/\tau_2'$ versus $\upsilon_{\mathrm{K-K_2}}[\mathrm{K}]$ can be fitted by a straight line, Γ is the natural radiative rate, $\sigma_i = k_i/\upsilon_{\mathrm{K-K_2}}$ is the total cross section for deactivation, $\upsilon_{\mathrm{K-K_2}} = (8kT/\pi\mu)^{1/2}$ is the Maxwellian averaged relative velocity for K-K_2, T is the cell temperature, μ is the reduced mass. The total cross section $\sigma_3 + \sigma_4$ is determined by the slope, and the natural radiative rate Γ_2 is obtained from the intercept of Eq. (13). The time-resolved fluorescence from the $^3\Lambda_g \to 1^3\sum_u^+$ (484 nm) can be treated as a difference between two exponential functions of Eq. (12). Here τ_1' can be obtained by the experimental curve fitting in different [K], Γ_1 and $\sigma_{-3} + \sigma_6$ can be obtained from the Stern–Volmer equation $1/\tau_1' = \Gamma_1 + (\sigma_{-3} + \sigma_6)\upsilon_{\mathrm{K-K_2}}[\mathrm{K}]$. Equations (11) and (12) can be integrated and the ratios of the time-integrated fluorescence intensities are expressed as

$$\frac{I_2/\varepsilon_2}{I_1/\varepsilon_1} = \frac{\Gamma_2 h\nu_2}{\Gamma_1 h\nu_1}\left(\frac{\Gamma_1}{\sigma_3\upsilon_{\mathrm{K-K_2}}[\mathrm{K}]} + \frac{\sigma_{-3} + \sigma_6}{\sigma_3}\right), \tag{14}$$

where ε is the efficiency of the detection system (including effects due to the photomultiplier, monochromator grating, and any filters used); the ratio of fluorescence intensity versus $1/\upsilon_{\mathrm{K-K_2}}[\mathrm{K}]$ can be fitted by a straight line, σ_3 is determined by the slope, and $\sigma_{-3} + \sigma_6$ is obtained from the intercept in the experimental result.

The cell temperature was fixed, and N_2 gas with variable pressure was filled in the cell. From Eqs. (9) and (10), the ratios of time-integrated fluorescence intensities at different [N_2] are expressed as

$$\begin{aligned}\frac{i_1/\varepsilon_1}{i_2/\varepsilon_2} = &\{\Gamma_1 h\nu_1(\sigma_3\upsilon_{\mathrm{K-K_2}}[\mathrm{K}] + \sigma_1\upsilon_{\mathrm{K-N_2}}[\mathrm{N_2}])\} \\ &\times \{\Gamma_2 h\nu_2(\Gamma_1 + (\sigma_{-3} + \sigma_6)\upsilon_{\mathrm{K-K_2}}[\mathrm{K}] \\ &+ (\sigma_{-1} + \sigma_5)\upsilon_{\mathrm{K-N_2}}[\mathrm{N_2}])\}^{-1},\end{aligned} \tag{15}$$

where [K] is invariable for the fixed temperature and [N_2] is variable, Γ_1, Γ_2, σ_3, $(\sigma_{-3} + \sigma_6)$ have been obtained from the front results, σ_1 and $(\sigma_{-1} + \sigma_5)$ can be determined by fitting the ratios of fluorescence intensities with Eq. (15).

The experimental setup was described previously.[15] The pure potassium metal was deposited in a cylindrical glass cell with inner diameter 2 cm and length 10 cm. The cell was sealed after baking and evacuating until a vacuum of 10^{-4} Pa was reached. The cell was connected to a vacuum system and filled with N_2 gas with variable pressure. The cell was placed inside an oven with four quartz windows, which was heated with resistive heater tapes. The temperature of the cell was measured with thermocouples. The densities of K atoms were determined from spectroscopy by the white-light absorption measurement in the blue wing of the self-broadened resonance D_2 line (766.5 nm).[16]

The OPO laser at wavelength 710 nm was used to excite K_2 molecules from the ground state $1^1\Sigma_g^+$ to $^1\Lambda_g$ state by two-photon absorption. The intensities of the time-resolved fluorescence from $^1\Lambda_g \to 1^1\sum_u^+$ (the direct fluorescence 650 nm) and $^3\Lambda_g \to 1^3\sum_u^+$ (the transfer fluorescence 484 nm) were recorded. The laser-induced fluorescence (LIF) signal was collected through a pair of lenses and focused onto the entrance slit of a monochromator and detected by the photomultiplier tube. The resulting time-resolved fluorescence was fed into a boxcar integrator, and then the date was stored in the computer for further treatment. The photon counter recorded the intensities of the time-integrated fluorescence, which were averaged over the whole signal in a period of time. The stray light and dark current were removed as a background. The wavelength-dependent detection system efficiency ε was measured using a calibrated tungsten-halogen lamp.

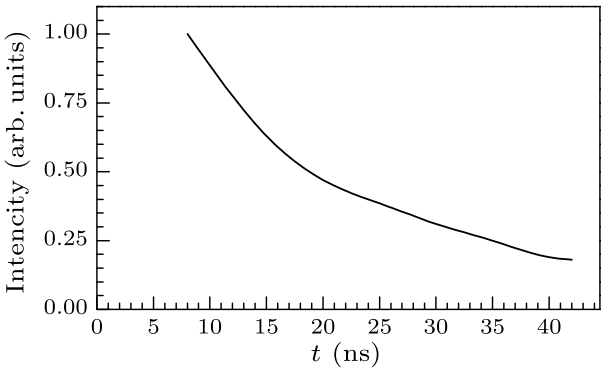

Fig. 2. Time-resolved fluorescence for K_2 in the $^1\Lambda_g \to 1^1\Sigma_u^+$ transition in pure K metal vapor.

In the pure potassium metal vapor, the cell temperature was fixed at 553 K. Figure 2 shows an exponential decay curve of the time-resolved fluorescence from the transition $^1\Lambda_g \to 1^1\sum_u^+$ (650 nm) and the effective lifetime is 19 ns.

The effective lifetimes for $^1\Lambda_g \rightarrow 1^1\Sigma_u^+$ were determined when the cell temperature was varied between 553 K and 753 K. According to the Stern–Volmer equation, the reciprocal of the effective lifetime τ_2' versus $\upsilon_{K-K_2}[K]$ can be fitted by a straight line. Figure 3 shows the experimental result, the total cross section $(\sigma_3 + \sigma_4)$ is $(2.5 \pm 0.6) \times 10^{-14}\,\mathrm{cm}^2$ from the slope and the radiative lifetime $(\tau_2'^0 = 1/\Gamma_2)$ is (20 ± 2) ns from the intercept.

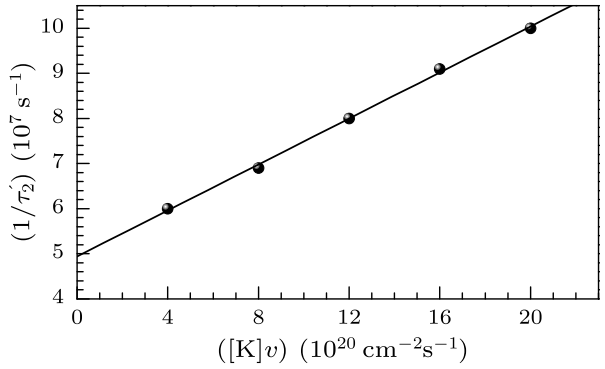

Fig. 3. Plot of the reciprocal of the effective lifetimes τ_2' against $([K]v)$.

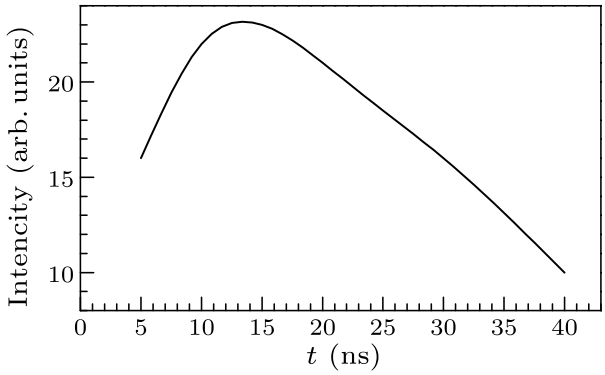

Fig. 4. Time-resolved fluorescence for K_2 in the $^3\Lambda_g \rightarrow 1^3\Sigma_u^+$ transition in pure K metal vapor.

Figure 4 shows the time-resolved fluorescence of K_2 in the $^3\Lambda_g \rightarrow 1^3\sum_u^+$ (484 nm) transition at a temperature of 553 K. According to Eq. (12), a difference between two exponential functions generated a maximal value feature as shown in Fig. 4. The effective lifetime τ_1' is (10.0 ± 1.5) ns by fitting of Fig. 4.

Figure 5 shows the resulting plot of $1/\tau_1'$ against $\upsilon_{K-K_2}[K]$. The total cross section $(\sigma_{-3} + \sigma_6)^{rev}$ is $(2.0 \pm 0.4) \times 10^{-14}\,\mathrm{cm}^2$ from the slope and the radiative lifetime $(\tau_1'^0 = 1/\Gamma_1)$ is (16.0 ± 3.2) ns from the intercept. Here $(\sigma_{-3} + \sigma_6)^{rev}$ denotes the cross section obtained by the time-resolved fluorescence. The lifetime (16.0 ± 3.2) ns is consistent with the value of (18 ± 2) ns obtained by Wang and Jia.[17]

Figure 6 shows the relation between $(I_2/\varepsilon_2)/(I_1/\varepsilon_1)$ and $([K]v)^{-1}$. According to Eq. (14), the ratio of the time-integrated fluorescence intensities versus $([K]v)^{-1}$ can be fitted by a straight line. Here σ_3 is $(1.1 \pm 0.3) \times 10^{-14}\,\mathrm{cm}^2$ from the slope, $(\sigma_{-3} + \sigma_6)^{int}$ is $(2.1 \pm 0.7) \times 10^{-14}\,\mathrm{cm}^2$ from the intercept, $(\sigma_{-3} + \sigma_6)^{int}$ denotes the cross section obtained by the time-integrated fluorescence. From the experimental results, $(\sigma_{-3} + \sigma_6)^{rev}$ and $(\sigma_{-3} + \sigma_6)^{int}$ are consistent, so this fact proves that the experimental methods are self-consistent.

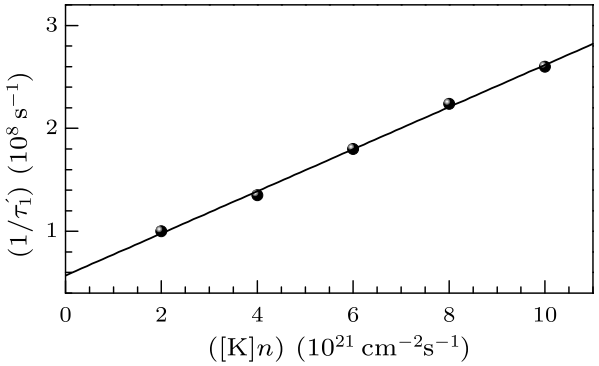

Fig. 5. Plot of the reciprocal of the effective lifetime τ_1' against $([K]v)$.

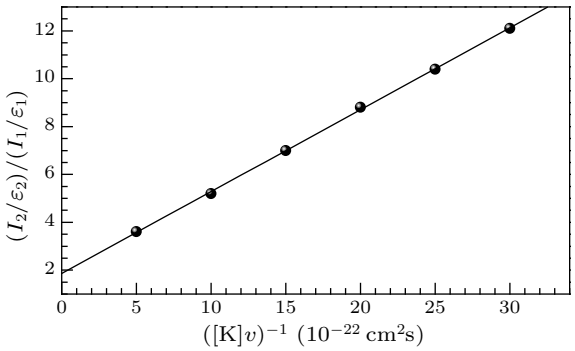

Fig. 6. Plot of the observed fluorescence ratio $(I_2/\varepsilon_2)/(I_1/\varepsilon_1)$ against $([K]v)^{-1}$.

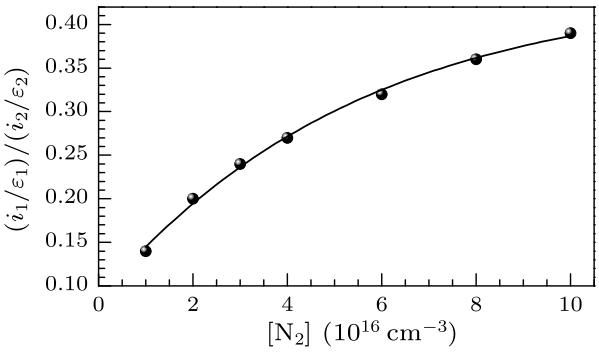

Fig. 7. Plot of the observed fluorescence ratio $(i_1/\varepsilon_1)/(i_2/\varepsilon_2)$ against $[N_2]$.

The cell temperature was fixed at 553 K and the system was filled with N_2 between 40 Pa and 400 Pa, the time-integrated direct fluorescence (650 nm) and transfer fluorescence (484 nm) intensities were measured, respectively. Figure 7 shows the plot of the observed fluorescence intensity ratio versus $[N_2]$. From the least-square fit through the experimental points, the values are found to be $\sigma_1 = (3.8 \pm 1.5) \times 10^{-15}\,\mathrm{cm}^2$ and $\sigma_{-1} + \sigma_5 = (8.9 \pm 3.5) \times 10^{-15}\,\mathrm{cm}^2$.

Estimates of the uncertainty in our measured σ_1 and $\sigma_{-1} + \sigma_5$ can be obtained from Eq. (15). The ratios of fluorescence intensities probably have an uncertainty of as much as 8%. The uncertainty in the ratio of the detection system efficiency is estimated to be 5%, while the uncertainty in the K density is estimated to be 8%. Γ_1 and Γ_2 are measured in our work and their uncertainties are estimated to be 20% and 10%, respectively. Here σ_3 and $(\sigma_{-3} + \sigma_6)$ are measured too and the corresponding uncertainties are estimated to be 25% and 20%. Considering all these various sources of statistical uncertainty stated above, the uncertainties for σ_1 and $(\sigma_{-1} + \sigma_5)$ are estimated to be 40%.

From the relation of $\sigma_1/\sigma_{-1} \propto \exp(\Delta E/kT)$, $\Delta E \sim 120\,\mathrm{cm}^{-1}$ is the wavenumber difference between the $^1\Lambda_g$ and $^3\Lambda_g$ states; σ_{-1} is estimated to be $2 \times 10^{-15}\,\mathrm{cm}^2$. A process analogous to the treatment described above may be employed to obtain σ_{-3}, then $\sigma_{-3} = 8 \times 10^{-15}\,\mathrm{cm}^2$. Therefore, $k_{-1}[\mathrm{N_2}] + k_{-3}[\mathrm{K}] \ll 1/\tau_2$ can be set up for our experimental conditions, and $k_{-1}[\mathrm{N_2}] + k_{-3}[\mathrm{K}]$ (the second term of the right section in Eq. (7)) can be neglected.

In conclusion, in a K-N_2 mixture, the cross sections for $K_2(^1\Lambda_g) \rightarrow K_2(^3\Lambda_g)$ and $K_2(^3\Lambda_g)$ collisions with N_2 at 553 K are $(3.8 \pm 1.5) \times 10^{-15}\,\mathrm{cm}^2$ and $(8.9 \pm 3.5) \times 10^{-15}\,\mathrm{cm}^2$, respectively. To our knowledge, this is the first report on the data of the cross sections for these processes.

References

[1] Hattaway B C et al 2004 *J. Chem. Phys.* **120** 1739
[2] Polly R et al 1996 *Chem. Phys. Lett.* **249** 174
[3] Zhou B and Li S M 2009 *Chin. Phys. Lett.* **26** 043401
[4] ShenY F et al 2006 *Chin. Phys. Lett.* **23** 1173
[5] Flynn G W, Parmenter C S and Wodtke A M 1996 *J. Phys. Chem.* **100** 12817
[6] Fecko C J, Freedman M A and Stephenson J A 2001 *J. Chem. Phys.* **115** 4132
[7] Niu Y Y, Wang R, Liu L and Cong S L 2007 *Chin. Phys. Lett.* **24** 3400
[8] Figl C et al 2004 *J. Chem. Phys.* **121** 11068
[9] Luo Y L, Lin K C, Liu D K and Liu H J 1992 *Phys. Rev.* A **46** 3834
[10] MA J et al 2007 *Chin. Phys. Lett.* **24** 1904
[11] Chang H C, Luo Y L and Lin K C 1991 *J. Chem. Phys.* **94** 3529
[12] Chang Y P et al 2008 *J. Chem. Phys.* **128** 234309
[13] ShenY F et al 2005 *Chin. Phys. Lett.* **22** 2805
[14] Magnier S and Millie Ph 1996 *Phys. Rev.* A **54** 204
[15] Zhang Y W et al 2009 *Chin. J. At. Mol. Phys.* **26** 859 (in Chinese)
[16] Vadla C, Knezovic S and Movre M 1992 *J. Phys.* B **25** 1337
[17] Wang G and Jia S T 1995 *Chin. J. At. Mol. Phys.* **12** 299 (in Chinese)